Preprints.org

Article

Not peer-reviewed version

Dynamic Correlations in Disordered Systems: Implications on High-Temperature Superconductivity

Takeshi Egami *

Posted Date: 15 December 2023

doi: 10.20944/preprints202312.1179.v1

Keywords: superconductivity; liquid and glass; dynamic correlation; disorder

Preprints.org is a free multidiscipline platform providing preprint service that is dedicated to making early versions of research outputs permanently available and citable. Preprints posted at Preprints.org appear in Web of Science, Crossref, Google Scholar, Scilit, Europe PMC.

Copyright: This is an open access article distributed under the Creative Commons Attribution License which permits unrestricted use, distribution, and reproduction in any medium, provided the original work is properly cited.

Preprints (www.preprints.org) | NOT PEER-REVIEWED | Posted: 15 December 2023 doi:10.20944/preprints202312.1179.v1

Disclaimer/Publisher's Note: The statements, opinions, and data contained in all publications are solely those of the individual author(s) and contributor(s) and not of MDPI and/or the editor(s). MDPI and/or the editor(s) disclaim responsibility for any injury to people or property resulting from any ideas, methods, instructions, or products referred to in the content.

Article

Dynamic Correlations in Disordered Systems: Implications on High-Temperature Superconductivity

Takeshi Egami [1,2]

[1] Shull-Wollan Center, Department of Materials Science and Engineering, and Department of Physics and Astronomy, University of Tennessee, Knoxville, TN 37996, USA; egami@utk.edu

[2] Materials Sciences and Technology Division, Oak Ridge National Laboratory, Oak Ridge, TN 37831, USA

Abstract: Liquid and gas are distinct in their extent of dynamic atomic correlations; in gas atoms are almost uncorrelated whereas they are strongly correlated in liquid. This distinction applies also to electronic systems. Fermi liquids are actually gas-like, whereas strongly correlated electrons are liquid-like. Doped Mott insulators share characteristics with supercooled liquids. Such distinctions have important implications on superconductivity. We discuss the evolution of dynamic atomic correlations in liquid with temperature, and a possible effect of dynamic correlations on the high-temperature superconductivity in the cuprates.

Keywords: superconductivity; liquid and glass; dynamic correlation; disorder

1. Introduction

At ambient pressure liquid evaporates to gas through a first-order phase transition. Under high pressure, however, the change becomes continuous beyond the tri-critical point. Thus, the distinction between liquid and gas is not as obvious as it may appear. But, the critical difference can be found in the specific heat, C_V. In ideal gas $C_V = (3/2)k_B$, whereas in liquid $C_V = 3\ k_B$ [1,2]. This is because atoms in gas interact with each other only through occasional collisions, so that the potential energy, $\langle U \rangle$, is practically zero. Thus, specific heat originates only from the kinetic energy, $\langle T \rangle$, and $C_V = (3/2)k_B$. On the other hand, atoms in liquid are always influencing each other through the interatomic potential. Thus, through the equipartition theorem $\langle U \rangle = \langle T \rangle$, resulting in $C_V = 3k_B$, known as Dulong-Petit law for solid. In other words, liquid is condensed matter, not high-density gas. Indeed, the physical density of liquid is almost as high as that of a solid [3]. In gas atom-atom interactions are collisional. In liquid atoms are held together by cohesive force just as solid, and atomic motions are vibrational [4].

In spite of such important differences between liquid and gas, many ideas and theories of liquid are based upon models of high-density gas. For instance, the hard-sphere (HS) model [5, 6] is a gas model with $\langle U \rangle = 0$. Widely used concepts, such as free-volume [7] and jamming [8], stem from the HS model, thus assume liquid basically as high-density gas. The widely used Weeks-Chandler-Andersen (WCA) principle [9] states that at high temperatures only the repulsive part of the potential is relevant, thus the HS model is always justified. Here, the role of the potential is essentially neglected. However, as we discuss below, the potential energy plays a critical role in controlling the properties of liquid and supercooled liquid.

Because there are fundamental and qualitative differences between the gas model and the elastic liquid/solid model, we should start with an elastic model in which the harmonic interaction is assumed from the beginning, instead of starting with the gas model and increasing density to describe liquid. Such an approach, based on the concept of atomic-level stresses [10] and the density wave instability [11], had a major success in describing the evolution of the structure of liquid with temperature [12] and in elucidating the glass transition [13]. In this paper we briefly describe this theory, discuss the atomic dynamics in superfluid ^{4}He observed by inelastic neutron scattering [14], and the possible implication on the high-temperature superconductivity in the cuprates [15].

© 2023 by the author(s). Distributed under a Creative Commons CC BY license.

Preprints (www.preprints.org) | NOT PEER-REVIEWED | Posted: 15 December 2023 doi:10.20944/preprints202312.1179.v1

2. Dynamic Correlation in Liquid and the Glass Transition

In 1952 Frank [16] suggested that icosahedral clusters of atoms (Figure 1) may exist in liquid, to explain the high degree of supercooling observed by Turnbull [17]. He argued that for the Lennard-Jones potential, the icosahedral cluster has a lower energy than the close-packed *f.c.c.* cluster, by 8.4%. The icosahedral cluster cannot be the basis of a simple crystalline phase because of the predominant five-fold symmetry, whereas it can exist as a short-range order (SRO) in an aperiodic structure of liquid. Frank argued that for this reason crystallization requires significant structural reorganization, and this presents the energy barrier for transformation [16]. Soon, Bernal discovered a high density of icosahedral clusters in his random-packed HS model [5]. Since then, the idea of regarding the icosahedral cluster, or similar high-symmetry clusters, as the building block to form a liquid structure became the standard approach to the structure of liquid [18–24]. However, this "bottom-up" approach cannot readily explain strong medium-range order (MRO) in the liquid structure.

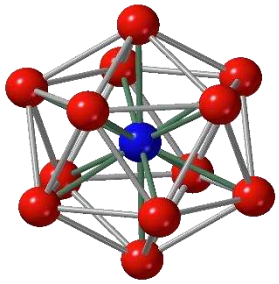

Figure 1. An icosahedral cluster.

The structure of liquid and glass is usually expressed in terms of the atomic pair-distribution function (PDF), $g(r)$, or $G(r) = 4\pi r\rho_0[g(r) - 1]$, where ρ_0 is the atomic number density [6], given by

$$g(r) = \frac{1}{N}\sum_{i,j}\delta\left(r - \left|\boldsymbol{r_i} - \boldsymbol{r_j}\right|\right). \quad (1)$$

where $\boldsymbol{r_i}$ is the position of the *i*-th atom and *N* is the total number of atoms. The PDF describes only the two-body correlation, whereas the full description of the real structure requires high-order correlations as well. However, the PDF can be directly determined by scattering experiment with x-ray or neutrons [25]. The PDF of metallic liquids and glasses show prominent exponentially decaying oscillations around the average density with a well-defined periodicity (Figure 2 [26]). The length-scale for the exponential decay, ξ_s,

$$G(r) = G_0(r)exp\left(-r/\xi_s\right), \quad (2)$$

obeys the Curie-Weiss law in its temperature dependence [12,26],

$$\xi_s(T) = \frac{C}{T - T_{IG}} \quad . \quad (3)$$

This diverges at T_{IG}, although it never happens because $T_{IG} < 0$. The state reached by extrapolation to T_{IG} is characterized by the long-range density wave correlation [11,26].

Preprints (www.preprints.org) | NOT PEER-REVIEWED | Posted: 15 December 2023 doi:10.20944/preprints202312.1179.v1

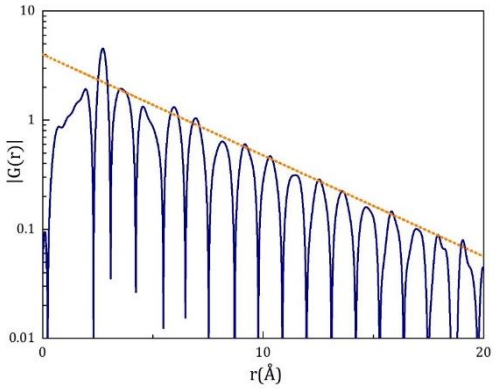

Figure 2. The $|G(r)|$ of $Pd_{42.5}Ni_{7.5}Cu_{30}P_{20}$ liquid at T = 600K, just above T_g [26].

Equation (2) suggests that there is a driving force toward this state, the density wave (DW) state. The right theoretical framework to study this state is the density wave theory, in which the atomic density, $\rho(\boldsymbol{r})$, is given by,

$$\rho(\boldsymbol{r}) = \int \rho(\boldsymbol{q}) e^{i\boldsymbol{q}\cdot\boldsymbol{r}} d\boldsymbol{q}. \quad (4)$$

Now, the Fourier-transform of the interatomic potential, $\phi(\boldsymbol{r})$, is strongly dependent upon the diverging part of the potential close to $\boldsymbol{r}$ = 0. However, the diverging part is never relevant, because atoms do not come so close to each other. Therefore, we can remove the diverging part to define the pseudopotential, $\phi_{pp}(\boldsymbol{r})$. Its Fourier-transform, $\phi_{pp}(\boldsymbol{q})$, was found to have a strong minimum close to the wavenumber expected for the DW state, $\boldsymbol{q_{DW}}$. Thus, we theorize that $\phi_{pp}(\boldsymbol{q})$ is driving the system to the DW state, resulting in the increase in ξ_s as temperature is reduced [11,27,28]. However, the SRO of the DW state was found to be quite poor, with almost no icosahedral local structure [26]. Therefore, the DW state, obtained by minimizing the energy in $\boldsymbol{q}$ space, and the SRO, obtained by minimizing the energy in $\boldsymbol{r}$ space, are incompatible with each other. Also, local thermal fluctuations disrupt the long-range nature of the DW state. Our theory is that the compromise among these competing factors produces the MRO [11,27,28]. This approach elucidates the Curie-Weiss law, Equation (2), and the glass transition temperature [13] with high quantitative accuracy for metallic glasses, and provides reasonable explanation of other properties [29,30].

3. Dynamic Correlation in Superfluid ^{4}He

We now turn our focus to the atomic dynamics in ^{4}He which becomes superfluid due to the Bose-Einstein (BE) condensation. The BE condensation is well-defined for ideal gas, whereas He atoms interact through the Lennard-Jones potential. As a result, only about 7% of He atoms condense to the BE state [31]. Thus, the PDF of ^{4}He determined by neutron scattering which shows the average interatomic distance of 3.6 Å [32] describes essentially the structure of uncondensed atoms. To determine the structure of the BE condensed atoms we measured the dynamic structure factor, $S(\boldsymbol{q}, E)$, of ^{4}He by inelastic neutron scattering, and transformed it to the energy-resolved PDF, $g(\boldsymbol{r}, E)$ [14] defined by.

$$g(r,E) = \frac{1}{N}\sum_{i,j}\int \delta\left(r - \left|\boldsymbol{r_i}(0) - \boldsymbol{r_j}(\boldsymbol{t})\right|\right) exp(i\omega t) dt. \quad (5)$$

where $\boldsymbol{r_i}(t)$ is the position of the i-th atom at time t and $E = \hbar\omega$.

If we focus on the roton energy at 0.7 meV, we are primarily looking at condensed atoms. Particularly by comparing $g(\boldsymbol{r}, E)$ above and below the BE condensation temperature, T_{BE}, we can extract the atomic correlations in the condensate. We discovered that the interatomic distance for the BE condensed atoms is 4 Å [14], much longer than that of the uncondensed atoms [32]. To illustrate this difference we compare the total PDF (in red) against the integral of $g(\boldsymbol{r}, E)$ from E = 0.69 to 0.9 meV (in blue) in Figure 3. It is clear that upon the BE condensation the first peak shifts outward by

Preprints (www.preprints.org) | NOT PEER-REVIEWED | Posted: 15 December 2023 doi:10.20944/preprints202312.1179.v1

0.3 Å or more. We explained this difference in terms of atomic wavefunction overlap [15]. In the condensed state the wavefunctions of different atoms cannot overlap, because it would lead to level-splitting. To allow such hybridization for each pair of atoms the ground state has to be a macroscopic resonant state, just as the resonant valence bond (RVB) state [33]. For bosons like ^{4}He spin resonance into the spin singlet state is not required. However, slow dynamics will not allow the system to reach such a massive resonant ground state, just as the antiferromagnet stays in the Néel state even though the true quantum ground state is the resonant state [34]. The simplest alternative is to eliminate the wavefunction overlap by atoms becoming separated a little further. As a result, the interatomic distance is larger than in uncondensed state where small overlap is allowed, just as in the exchange hole compared to the correlation hole for electrons [35].

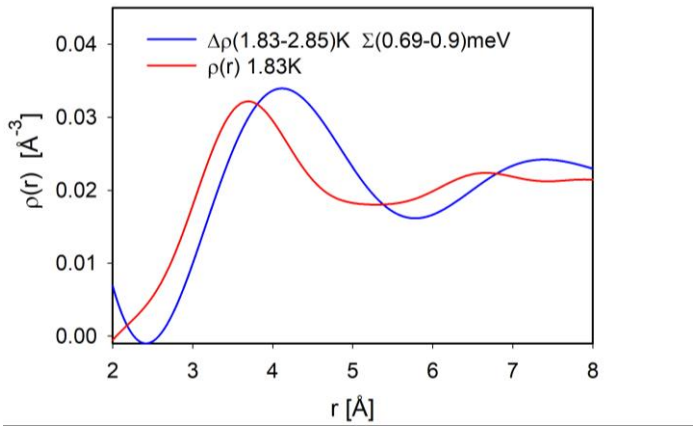

Figure 3. The total PDF (red) and the portion (0.69 – 0.9 meV) of the difference in the energy-resolved PDFs of ^{4}He, $\Delta g(r, E) = g_{T1}(r, E) - g_{T2}(r, E)$ (blue), for $T1$ = 1.83 K and $T2$ = 2.85 K [14].

4. Dynamic Correlation among Electrons

Our method to observe dynamic correlations in real space and time using the energy-resolved PDF [14] and the Van Hove function [36,37],

$$G(r,t) = \frac{1}{N}\sum_{i,j}\delta\left(r - \left|\boldsymbol{r_i}(0) - \boldsymbol{r_j}(\boldsymbol{t})\right|\right), \qquad (6)$$

can be applied to electrons to observe dynamic correlations among electrons. For atoms the classical interpretation of the correlation functions, eqs. (1), (5) and (6), are valid, but for electrons we have to be more careful about the quantum effect. The inelastic x-ray scattering cross-section of electrons is given by [38],

$$\frac{d\sigma}{d\omega d\Omega} = \sigma_0 S(q,\omega) = \frac{\sigma_0}{2\pi}\sum_{\boldsymbol{k},\boldsymbol{k'}}\int \langle c_{\boldsymbol{k}}^{+}(t)c_{\boldsymbol{k}+\boldsymbol{q}}(t)c_{\boldsymbol{k'}+\boldsymbol{q}}^{+}(0)c_{\boldsymbol{k'}}(0)\rangle\, e^{-i\omega t}dt, \qquad (7)$$

where $c_{\boldsymbol{k}}^{+}(t)$ creates a fermion with the momentum $\boldsymbol{k}$ at time t, $\sigma_0 = e^2/m$, e is the electron charge, m is the electron mass, and <…> denotes quantum and thermal average. Usually, the decoupling by random-phase approximation (RPA),

$$\langle c_{\boldsymbol{k}}^{+}(t)c_{\boldsymbol{k}+\boldsymbol{q}}(t)c_{\boldsymbol{k'}+\boldsymbol{q}}^{+}(0)c_{\boldsymbol{k'}}(0)\rangle \rightarrow \langle c_{\boldsymbol{k}+\boldsymbol{q}}(t)c_{\boldsymbol{k'}+\boldsymbol{q}}^{+}(0)\rangle\langle c_{\boldsymbol{k}}^{+}(t)c_{\boldsymbol{k'}}(0)\rangle, \qquad (8)$$

is applied and,

$$\langle c_{\boldsymbol{k}+\boldsymbol{q}}(t)c_{\boldsymbol{k'}+\boldsymbol{q}}^{+}(0)\rangle\langle c_{\boldsymbol{k}}^{+}(t)c_{\boldsymbol{k'}}(0)\rangle = \delta_{\boldsymbol{k},\boldsymbol{k'}}\left(1 - n_{\boldsymbol{k}+\boldsymbol{q}}\right)n_{\boldsymbol{k}}\delta\left(\omega - \left(E_{\boldsymbol{k}+\boldsymbol{q}} - E_{\boldsymbol{k}}\right)/\hbar\right)e^{i\omega t} \qquad (9)$$

where $n_{\boldsymbol{k}} = \langle c_{\boldsymbol{k}}^{+}c_{\boldsymbol{k}}\rangle$. Thus, the dynamic structure factor, $S(\boldsymbol{q}, \omega)$, describes the excitation of electrons from below the Fermi level to above. It is also interpreted as the imaginary part of the dielectric response function [39].

However, the RPA decoupling in reciprocal space erases the phase relationship between the initial and final states in the transition, which contains the information on the real space correlations. To avoid this loss of phase information and to observe the correlation in real space, we introduce a real-space description,

Preprints (www.preprints.org) | NOT PEER-REVIEWED | Posted: 15 December 2023 doi:10.20944/preprints202312.1179.v1

$$c_{\boldsymbol{k}}^{+}(t) = \int c^{+}(\boldsymbol{r}',t)e^{-i\boldsymbol{k}\cdot\boldsymbol{r}'}\,d\boldsymbol{r}', \quad c_{\boldsymbol{k}+\boldsymbol{q}}(t) = \int c(\boldsymbol{r}'',t)e^{i(\boldsymbol{k}+\boldsymbol{q})\cdot\boldsymbol{r}''}\,d\boldsymbol{r}'' \quad . \tag{10}$$

where $c^{+}(\boldsymbol{r},t)$ is a fermion creator at $\boldsymbol{r}$ and t. Then,

$$c_{\boldsymbol{k}}^{+}(t)c_{\boldsymbol{k}+\boldsymbol{q}}(t)c_{\boldsymbol{k}'+\boldsymbol{q}}^{+}(0)c_{\boldsymbol{k}'}(0) = \int c^{+}(\boldsymbol{r}',t)c(\boldsymbol{r}'',t)c^{+}(\boldsymbol{r}''',0)c(\boldsymbol{r}'''',0)\times$$
$$exp(i[-\boldsymbol{k}\cdot\boldsymbol{r}' + (\boldsymbol{k}+\boldsymbol{q})\cdot\boldsymbol{r}'' - (\boldsymbol{k}'+\boldsymbol{q})\cdot\boldsymbol{r}''' + \boldsymbol{k}'\cdot\boldsymbol{r}'''']) d\boldsymbol{r}'d\boldsymbol{r}''d\boldsymbol{r}'''d\boldsymbol{r}''''. \tag{11}$$

The intermediate scattering function [40],

$$F(\boldsymbol{q},t) = \int S(q,\omega)e^{i\omega t}d\omega, \tag{12}$$

is given by,

$$F(\boldsymbol{q},t) = \sum_{\boldsymbol{k},\boldsymbol{k}'}\langle c_{\boldsymbol{k}}^{+}(t)c_{\boldsymbol{k}+\boldsymbol{q}}(t)c_{\boldsymbol{k}'+\boldsymbol{q}}^{+}(0)c_{\boldsymbol{k}'}(0)\rangle. \tag{13}$$

In the real space representation, Equation (11), the summation over $\boldsymbol{k}$ and $\boldsymbol{k}'$ in Equation (13) yields $\boldsymbol{r}' = \boldsymbol{r}''$, $\boldsymbol{r}''' = \boldsymbol{r}''''$. Then,

$$F(\boldsymbol{q},t) = \int \langle c^{+}(\boldsymbol{r}',t)c(\boldsymbol{r}',t)c^{+}(\boldsymbol{r}''',0)c(\boldsymbol{r}''',0)\rangle exp\big(i\boldsymbol{q}\cdot(\boldsymbol{r}'-\boldsymbol{r}''')\big)d\boldsymbol{r}'d\boldsymbol{r}'''$$
$$= \int \langle \rho(\boldsymbol{r}',t)\rho(\boldsymbol{r}''',0)\rangle exp\big(i\boldsymbol{q}\cdot(\boldsymbol{r}'-\boldsymbol{r}''')\big)d\boldsymbol{r}'d\boldsymbol{r}''', \tag{14}$$

where

$$\rho(\boldsymbol{r},t) = c^{+}(\boldsymbol{r},t)c(\boldsymbol{r},t) \tag{15}$$

is the local density operator. Thus, the Van Hove function is expressed as the density correlation function in real space and time,

$$G(\boldsymbol{r},t) = \int F(\boldsymbol{q},t)e^{i\boldsymbol{q}\cdot\boldsymbol{r}}d\boldsymbol{q} = \int \langle \rho(\boldsymbol{r}+\boldsymbol{r}',t)\rho(\boldsymbol{r}',0)\rangle d\boldsymbol{r}'. \tag{16}$$

This proves that the classical interpretation of the double-Fourier-transformation of $S(\boldsymbol{q}, E)$ as the Van Hove correlation function is valid, even for electrons. The energy-resolved PDF is given by,

$$g(r,\omega) = \frac{1}{2\pi}\int G(r,t)e^{-i\omega t}dt. \tag{17}$$

We measured the electronic $S(\boldsymbol{q}, E)$ for polycrystalline beryllium by inelastic x-ray scattering with the incident energy of 11.32 keV and energy resolution of 0.7 eV at the Beamline 27ID-B of the Advanced Photon Source of Argonne National Laboratory. The preliminary result [41] shows the exchange-correlation hole of the size about 2 Å. Surprisingly, at the plasmon energy of about 20 eV the exchange-correlation hole is extended to about 5 Å. In plasmon electrons are dynamically correlated, resulting in larger separation among electrons than in electrons at large. This result demonstrates that the dynamic state affects electron correlations. The details of this observation will be reported elsewhere.

5. Implication on High-Temperature Superconductivity

The combination of the result on ^{4}He and the observation of electron correlations by inelastic x-ray scattering have very significant implications on the high-temperature superconductivity of the cuprates. In the regular BCS superconductors electrons are in the Fermi-liquid state, and they are gas-like as discussed above. Electrons avoid each other by forming exchange-correlation holes, and the density functional theory (DFT) [42] works. The Cooper pairs are large and they B-E condensate at high temperatures of the order of 1000K. Thus, the pairing temperature determines the superconducting critical temperature, T_c. The Cooper pairs are large, up to 1000Å, and they are strongly overlapping with each other.

In contrast, in the cuprates electrons are strongly correlated, just as in liquid and supercooled liquid in which the potential energy is as important as the kinetic energy. For this reason, it is interesting to note that it was recently found that in the overdoped cuprates the periodicity of the charge density wave was independent of the Fermi momentum as the doping density was changed [43]. It is likely that the Coulomb repulsion energy is involved in the formation of the density waves, for instance through the pseudopotential discussed above [11,27,28].

Preprints (www.preprints.org) | NOT PEER-REVIEWED | Posted: 15 December 2023 doi:10.20944/preprints202312.1179.v1

Furthermore, in the cuprates the Cooper pairs are small, of the order of nm in size, and low in density. Thus, they are likely to be preformed above the superconducting transition temperature [44-46]. If that is the case, T_c is equal to T_{BE}, and it is controlled by the BE condensation rather than by pairing. We speculate that as in the case of ^{4}He the separation between Cooper pairs is longer in the BE condensate than in the normal state, to avoid wavefunction overlap. Then the Coulomb repulsion energy is reduced in the BE condensate compared to the normal state, adding to the driving force for the BE condensation [15]. The difference is similar to the case of exchange and correlation effects for fermions, so the energy difference must be related to the exchange constant. This effect is most likely negligible for ^{4}He, because the interaction energy (van der Waals force) is small. However, for the cuprates a small change in the repulsion energy can have a very significant effect. Because the hole density is low, the energy associated with wavefunction overlap is a small percentage of U. Nevertheless, the on-site Coulomb repulsion, U, is nearly 10 eV at Cu [35], huge in contrast to k_BT_c ~ 10 meV. Although the value of U itself may not be influenced by the BE condensation, slight changes in the extent of the *p-d* hybridization due to the BE condensation can affect the total repulsion energy. Thus, a tiny change in the repulsion energy can have a major effect on T_c. So far, the effort to increase T_c focused on the pairing force. This new mechanism calls for a change in strategy, to increase T_c through the correlation effects.

To test this hypothesis we plan to measure the $g(\mathbf{r}, E)$ for doped holes in the superconducting cuprates with inelastic x-ray scattering. The measurement is quite difficult because of the low intensity of the signal due to the high energy-resolution (better than 10 meV) required to observe the energy gap, and due to low doping density. However, this is within the realm of feasibility with advanced facilities.

6. Conclusions

Gas and liquid are fundamentally different in the role of the interatomic potential. In gas atomic interactions are collisional and the average potential energy is negligibly small compared to the kinetic energy. In liquids the potential energy is as important as the kinetic energy. We suggest that this difference can be instructive in discussing the difference in dynamics between nearly free electrons and strongly correlated electrons. We point out that electron correlation can be influenced by the dynamic state of electrons. In particular, the Bose-Einstein condensation of Cooper pairs could affect electron correlation, giving rise to an additional driving force to increase the superconducting transition temperature.

Funding: This work was supported by the U. S. Department of Energy, Office of Science, Basic Energy Sciences, Materials Science and Engineering Division.

Data Availability Statement: Data used in this work are available upon request from the corresponding author.

Acknowledgments: The author is grateful to Peter Fulde for encouragement.

Conflicts of Interest: The author declares no conflict of interest.

Notice of Copyright: This manuscript has been authored by UT-Battelle, LLC under Contract No. DE-AC05-00OR22725 with the U.S. Department of Energy. The United States Government retains and the publisher, by accepting the article for publication, acknowledges that the United States Government retains a non-exclusive, paid-up, irrevocable, world-wide license to publish or reproduce the published form of this manuscript, or allow others to do so, for United States Government purposes. The Department of Energy will provide public access to these results of federally sponsored research in accordance with the DOE Public Access Plan (http://energy.gov/downloads/doe-public-access-plan).

References

1. Wallace, D.C. Statistical mechanics of monoatomic liquids. *Phys. Rev. E* **1997,** 56, 4179-4186.
2. Wallace, D.C. Liquid dynamics theory of high-temperature specific heat. *Phys. Rev. E* **1998,** 57, 1717-1722.
3. Egami, T. Understanding the Properties and Structure of Metallic Glasses at the Atomic Level. *J. Metals*, **2010,** 62, 2, 70-75.
4. Moon, J.; Lindsay, L.; Egami, T. Atomic dynamics in fluids: Normal mode analysis revisited. *Phys. Rev. E* **2023,** 108, 014601.

Preprints (www.preprints.org) | NOT PEER-REVIEWED | Posted: 15 December 2023 doi:10.20944/preprints202312.1179.v1

5. Bernal, J.D. A geometrical approach to the structure of liquids. *Nature* **1959,** 183, 141-147.
6. Finny, J. Random packing and the structure of simple liquids. I. The geometry of random close packing. *Proc. Roy. Soc. Lond. A* **1970,** 319, 479-493.
7. Cohen, M.H.; Turnbull, D. Molecular transport in liquids and glasses. *J. Chem. Phys.* **1959,** 31, 1164-1169.
8. Liu, A.J.; Nagel, S.R. The jamming transition and the marginally jammed solid. *Ann, Rev. Cond. Mat.* 2010, 1, 347-369.
9. Weeks, J.D.; Chandler, D; Andersen, H.C. Role of repulsive forces in determining the equilibrium structure of simple liquids. *J. Chem. Phys.* **1971,** 54, 5237-5247.
10. Egami, T. Atomic level stresses. *Progr. Mater. Sci.* **2011,** 56, 637-653.
11. Egami, T.; Ryu, C.W. Structural principles in metallic liquids and glasses: Bottom-up or top-down. *Frontiers in Materials* **2022,** 9, 874191.
12. Egami, T.; Ryu, C.W. Medium-range atomic correlation in simple liquid. II. Theory of temperature dependence. *Phys. Rev. E* **2021,** 104, 064110.
13. Egami, T.; Poon, S.J.; Zhang, Z.; Keppens, V. Glass transition in metallic glasses: A microscopic model of topological fluctuations in the bonding network, *Phys. Rev. B* **2007,** 76, 024203.
14. Dmowski, W.; Diallo, S.O.; Lokshin, K.; Ehlers, G.; Ferré, G.; Boronat, J.; Egami, T. Observation of dynamic atom-atom correlation in liquid helium in real space, *Nature Commun.* **2017,** 8, 15294.
15. Egami, T. K. Alex Müller and superconductivity, *Physica C* **2023,** 613, 1354345.
16. Frank, F.C. Supercooling of liquids, *Proc. Roy. Soc. Lond. A* **1952,** 215, 43-46.
17. Turnbull, D. Kinetics of solidification of supercooled liquid mercury droplets, *J. Chem. Phys.* **1952,** 20, 411-424.
18. Sadoc, J.F. Use of regular polytopes for the mathematical description of the order in amorphous structures, *J. Non-Cryst. Solids* **1981, 44,** 17-30.
19. Sethna, J.P. Frustration and curvature: Glasses and the cholesteric blue phase, *Phys. Rev. Lett.* **1983,** 51, 2198-2201.
20. Nelson, D.R. Order, frustration, and defects in liquids and glasses, *Phys. Rev. B* **1983,** 28, 5515-5535.
21. Steinhardt, P.J.; Nelson, D.R.; Ronchetti, M. Icosahedral bond order in supercooled liquids, *Phys. Rev. Lett.* **1981,** 47, 1297-1300.
22. Tomida, T.; Egami, T. Molecular-dynamics study of orientational order in liquids and glasses and its relation to the glass transition. *Phys. Rev. B* **1995,** 52, 3290-3308.
23. Miracle, D.B. A structural model for metallic glasses, *Nature Mater*. **2004,** 3, 697-702.
24. Sheng, H.W.; Luo, W.K.; Alamgir, F.M.; Bai, J.M.; Ma, E. Atomic packing and short-to-medium-range order in metallic glasses, *Nature* **2006,** 439, 419-425.
25. Warren, B.E. *X-ray diffraction* (Addison-Wesley, Reading, 1969).
26. Ryu, C.W.; Dmowski, W.; Kelton, K.F.; Lee, G.W.; Park, E.S.; Morris, J.R.; Egami, T. Curie-Weiss behavior of liquid structure and ideal glass state. *Scientific Reports*, **2019,** 9, 18579.
27. Egami, T.; Ryu, C.W. World beyond the nearest neighbors. *J. Phys: Condens. Matter*, **2023,** 35, 174002.
28. Egami, T.; Ryu, C.W. Origin of medium-range atomic correlation in simple liquid: Density wave theory. *AIP Adv.* **2023,** 13, 085308.
29. Ryu, C.W.; Dmowski, W.; Egami, T. Ideality of liquid structure: A case study for metallic alloy liquids. *Phys. Rev. E*, **2020,** 101, 030601(R).
30. Ryu, C.W.; Egami, T. Origin of liquid fragility. *Phys. Rev. E*, **2020,** 102, 042615.
31. Glyde, H.R. *Excitations in liquid and solid helium*; Clarendon Press, Oxford, UK, 1994.
32. Svensson, E.C.; Sears, V.F.; Woods, A.D.B.; Martel, P. Neutron-diffraction study of the static structure factor and pair correlations in liquid ^{4}He. *Phys. Rev. B* **1980,** 21, 3538-3651.
33. Anderson P.W. *Science* **1987,** 235, 1196-1198.
34. Keffer, F. *Spin waves, in Handbuch der Physik, 18, pt. 2*; Springer-Verlag, Berlin, GE, 1966.
35. Fulde, P. *Electron correlations in molecules and solids*; Springer, Berlin, 2012.
36. Van Hove, L. Correlation in space and time and Born approximation scattering in systems of interacting particles. *Phys. Rev.* **1954,** 95, 249-262.
37. Egami, T.; Shinohara, Y. Perspective: Correlated atomic dynamics in liquid seen in real space and time. *J. Chem. Phys.* **2020,** 153, 180902.
38. *e.g.*, Platzman, P.M.; Tzor, N. X-ray scattering from electron gas. *Phys. Rev.* **1965,** 139, A410-A413.
39. Abbamonte, P.; Finkelstein, K.D.; Collins, M.D.; Gruner, S.M. Imaging density disturbances in water with a 41.3-attosecond time resolution. *Phys. Rev. Lett.* **2004,** 92, 237401.
40. Lovesey, S.W. *Theory of neutron scattering from condensed matter*; Oxford University Press, Oxford, UK, 1984.
41. Bista, R.; Upton, M.; Shinohara, Y.; Egami, T. Direct observation of electron correlation in space by inelastic x-ray scattering. **2023,** unpublished
42. Kohn, W.; Sham, L.J. Self-consistent equations including exchange and correlation effects. *Phys. Rev.* **1965,** 140, A1133-A1138.

Preprints (www.preprints.org) | NOT PEER-REVIEWED | Posted: 15 December 2023 doi:10.20944/preprints202312.1179.v1

43. Li, Q.; Huang, H.-Y.; Ren, T.; Weschke, E.; Ju, L.; Zou, C.; Zhang, S.; Qiu, Q.; Liu, J.; Ding, S.; Singh, A.; Prokhnenko, O.; Huang, D.-J.; Esterlis, I.; Wang, Y.; Xie, Y.; Peng, Y. Prevailing charge order in overdoped $La_{2-x}Sr_xCuO_4$ beyond the superconducting dome. *Phys. Rev. Lett*. **2023,** 131, 116002.
44. Emery, V.J.; Kivelson, S.A. Importance of phase fluctuations in superconductors with small superfluid density. *Nature* **1995,** 374 434-437.
45. Uemura, Y.J. Bose-Einstein to BCS crossover picture for high-T_c cuprates, *Physica C* **1997,** 282-287, 194-197.
46. Xu, Z.A.; Ong, N.P.; Wnag, Y.; Kakeshita, T.; Uchida, S. Vortex-like excitations and the onset of superconducting phase fluctuation in underdoped $La_{2-x}Sr_xCuO_4$. *Nature* **2000,** 406, 486-488.

Disclaimer/Publisher's Note: The statements, opinions and data contained in all publications are solely those of the individual author(s) and contributor(s) and not of MDPI and/or the editor(s). MDPI and/or the editor(s) disclaim responsibility for any injury to people or property resulting from any ideas, methods, instructions or products referred to in the content.